Astron. Astrophys. 362, 383–394 (2000)

ASTRONOMY AND ASTROPHYSICS

Moments of energetic particle distributions in the solar atmosphere

A.J. Conway

Department of Physics and Astronomy, The Open University, Walton Hall, Milton Keynes MK7 7AN, UK (a.j.conway@open.ac.uk)

Received 10 July 2000 / Accepted 22 August 2000

Abstract. This paper describes a theory that provides a direct link between observable properties of energetic particle distributions and the unobservable properties of the initial distributions. A general approach is first outlined and then applied to the specific situation of collisional electron transport in the solar atmosphere. By building on previous results, this treatment does not require explicit solution of the Fokker-Planck equation. In particular, we derive results for two important consequences of an energetic electron distribution: 1) The emission of hard X-ray bremsstrahlung radiation and 2) energy deposition in the background plasma by Coulomb collisions. For 1) we describe the energy spectrum of the emission completely and provide a description of its spatial and pitch angle properties in terms of the first and second order moments of the injected electron distribution. This means that for any assumed initial electron distribution, expressions are obtained that predict the HXR source's spatial position and extent for any photon energy. The results have most immediate application to phenomena associated with the early impulsive stage of solar flares involving energetic electrons. Other potential uses include: calculation of Hα impact polarisation; application to polarisational and directional properties of hard X-rays; and diagnostics of unobservably high energy features in the electron spectrum.

Key words: radiation mechanisms: non-thermal – Sun: flares – Sun: X-rays, gamma rays – Sun: corona

1. Introduction

Hard X-Ray (HXR) and radio emission from the Sun tells us that non-thermal distributions of electrons are present during the impulsive stage of a solar flare (Brown & Smith 1980). These electrons have energies (tens to hundreds of keV) much greater than the ambient particles of the solar atmosphere (< 10 keV), and there is good reason to believe their particle distributions are anisotropic and, in some cases, beam-like (Karlicky 1997). Careful interpretation of the HXR and radio observations of the impulsive stage of flares can lead us to a better understanding of how the energy is first released, then given to non-thermal particles, and then lost causing subsequent, more gradual solar flare phenomena. Observations of gamma-rays also tell us that protons and ions are accelerated during a flare, and that their total energy content is arguably similar to that of the electrons (Trottet et al. 1998; Ramaty et al. 1995). The work presented in this paper is primarily aimed at electrons, because they can produce HXRs which can be imaged, though many of the results presented here can be easily extended to describing protons.

The observation of coronal, impulsive HXR sources (Masuda et al. 1995) has been interpreted as being the most direct evidence yet of the location of a flare energy release site. It is plausible to make such an interpretation because the short collisional life-times of HXR producing electrons (relative to protons/ions that produce gamma-ray lines) mean that the HXRs they emit give us the earliest, and spatially nearest, information on where energy is being released. It is interesting to examine the assumptions implicit in the last sentence, they are that: 1) the acceleration of particles is localised in space and time (in the Masuda case to the loop-top), and 2) the electrons are not a secondary product of energy release, e.g. accelerated by ions or protons which were the first to receive energy. Possible scenarios exist that explain the observations with alternative assumptions that are equally plausible. For example, one possibility is that the energy is first released into waves, which then accelerate particles, e.g. Miller et al. (1997). Models invoking the existence of density pockets (Wheatland & Melrose, 1995) can then be used to explain the loop-top source, without energy release taking place there. The fact that the HXR source was clearly above the soft X-ray loop top is significant as it raises the problematic issue of energy transfer across magnetic field lines, as tentatively suggested by Conway & MacKinnon (1998b). (Note: A prior paper Conway & MacKinnon (1998a) proposes a model based on the erroneous result that electron-cyclotron maser emission can travel *along* magnetic field lines.) Regarding assumption 2 above, inferences made about the energy release site could well be wrong if electrons are not a primary product. Electron acceleration by protons or ions was found to be a natural consequence of a neutral beam (protons and electrons travelling together) by Karlicky et al. (2000), though this mechanism by itself cannot account for HXRs in larger flares due to energy efficiency constraints (Brown et al. 2000). It is clear that existing observations, and the observations that will be made by HESSI, need careful interpretation to yield information about how and where the particles were accelerated. Much of this interpretation is model dependent, but whatever the model, it must, at the very least, account for particle transport.

There are of course a great many effects to be considered when modelling particle transport. These range from straightforward propagation along the magnetic field, to complicated wave-particle interactions and instabilities. Indeed, the term “transport” could even include the particle acceleration itself. The formalism presented at the start of this paper provides a frame-work to address any of these effects in terms of moments of the distribution. Whether it is practical to do so is another matter, and depends on the availability of solution to stochastic differential equations. Such solutions are available for the case of an arbitrary density and constant magnetic field strength (Conway et al. 1998), and these are used to yield useful results in this paper. The use of the results and methods are two-fold. Firstly, it provides mathematical results that can be used to link observations and theory without recourse to detailed numerical simulations. Secondly, in more complicated cases (i.e. beyond effects of propagation and collisions) it can provide specific results that can be used to verify that the distributions from numerical simulations have the correct moments. We chose to concentrate our attention on propagation and collisional effects on this paper for two reasons. Firstly, the availability of simple mathematical results for this case, and also because these effects *must* be accounted for in nearly every interpretation of HXR observations. Other effects, such as stochastic particle acceleration, the electron-cyclotron maser and magnetic field convergence, are certainly of great interest, but there is no reason to suppose that they will be important in every flare. Further discussion of motivation of this work is discussed by Conway (2000).

Two physical properties of the solar atmosphere play a key rôle in particle transport. The first is the magnetic field which guides charged particles so that they ‘spiral’ along the field lines. The magnetic field does not directly affect the energy of a charged particle; it only alters the pitch angle in regions of changing field strength. The second key property is the density of the ‘cold’ (i.e. thermal energy $\ll$ energetic particle energy) background particles. As energetic particles move through a background media, they interact with its particles via the Coulomb force. At any given moment an energetic particle will experience collisions with a very large number of background particles. This has two implications. Firstly, it is a scattering process and must be treated statistically. This means that a particle with given velocity at some time, cannot have its velocity calculated uniquely for some later time. Secondly, because there are so many collisions per second, Coulomb collisions will change the velocity of the particle in a continuous way on observational timescales. That is, the change in a particle’s velocity in, say, a second, is not due to any single collision, but due to the effects of a great many collisions.

Coulomb collisions are regarded as distant, in the sense that the vast number of distant collisions, involving only small changes to E and μ, dominate over the few close encounters that produce large changes in these quantities (Spitzer 1962). However, the closer encounters are the ones that are important in producing the bremsstrahlung Hard X-rays, for the simple reason that an energy exchange of at least several keV is needed to produce a photon of several keV. The rate of HXR production and the rate of energy loss of an energetic electron are both proportional to a single physical quantity: the density of the background medium. This link between Coulomb collisions and HXR production is the reason why the concept of column depth is so useful. It is also the reason why it is actually more convenient to deal with moments of the HXR intensity distribution than it is to deal directly with the moments of the electron distribution. This is discussed in more detail below. The implication of this is that quantities of greatest observational interest, e.g. the moments describing the spatial location and extent of a HXR source, can be related directly to moments of the injected distribution without any need to solve the Fokker-Planck equation directly.

All previous descriptions of energetic particle distributions accounting for stochastic effects in the solar atmosphere have been numerical in nature (Leach & Petrosian 1981; Kovalev & Korolev 1981; Bai 1982; Hamilton et al. 1990; MacKinnon & Craig 1991). Analytic results that add valuable insight have also been developed over the last three decades, but, until now, only for the deterministic (i.e. mean) aspects of particle transport. The mean scattering approach, as it has been called, was first used by Brown (1971) and developed further by Emslie (1978), and later formulated and solved in a more general form, in terms of the continuity equation, by Vilmer et al. (1986) and Craig et al. (1985).

In this paper variations across the magnetic field are ignored, e.g. the background density and particle distribution are only considered as varying along the magnetic field lines. Basic physics and recent observations strongly suggest that such quantities can vary across field lines. Also, the time profile of hard X-rays may be thought to be composed of many individual spikes, with the time density of spikes being greatest at the HXR peak. Present HXR observations do not have sufficient spatial or temporal resolution to investigate these possibilities directly and so they are not considered in this paper. However, the theory presented here is not inconsistent with them, if quantities such as the density and particle distribution are thought of as averages across the field line, and over a length of time greater than the width of an elementary spike.

This paper’s main purpose is to provide mathematical expressions relating (directly and indirectly) observable moments, to the moments of the injected distribution. Sect. 2 sets out the general mathematical formalism. Sect. 3 considers results specific to HXR emission and energy deposition. Sect. 4 shows how to derive expressions for time-independent moments for the case of a non-uniform background density and constant magnetic field, and to derive temporal moments for the uniform density case. Sect. 5 discusses the implications and uses of the results.

2. General formalism

Consider a cross-section σ that describes a process involving an energetic charged particle of energy E, pitch angle cosine μ, that is at a distance s from some fixed reference point on a magnetic field line. We assume that a charged particle will follow a single field line, which is a good approximation in many astrophysical scenarios. The two specific cross-sections that we are concerned with in this paper are the Hard X-ray (HXR) bremsstrahlung cross-section and Coulomb energy loss cross-section.

Given the particle distribution function $f(E, \mu, s; t)$ (number of energetic electrons per unit E, per unit μ, per unit s at time t), the total rate of the process described by σ at time t, $I_\sigma(t)$, can be expressed:

$$I_\sigma(t) = \int_{-\infty}^{\infty} \int_{-1}^{1} \int_{0}^{\infty} \sigma n v f(E, \mu, s; t) dE d\mu ds \qquad (1)$$

where $n(s)$ is the density of background particles, and $v(E)$ is the speed of the energetic particle. (The semi-colon is used to emphasise that t is the independent variable, an issue that will become more important later. Hereafter, multiple integral symbols, integral limits and function arguments like those that appear in the above equation will be omitted for clarity, unless the specifically needed.) The definition of f is such that $I_\sigma(t) = \mathcal{N}(t)$ if $\sigma = 1/nv$, where $\mathcal{N}(t)$ is the number of particles in the whole system at time t. Note that $E = 0$ does not mean zero energy, it means that the particle has joined the thermal distribution and can no longer be described by the energetic particle Fokker-Planck equation.

Eq. (1) can be regarded as the zeroth time dependent moment of the distribution f weighted by the cross-section σ (we choose to phrase it this way to emphasise the physics - it could equally well be regarded as the zeroth moment of the distribution σf). More generally we can write that the time dependent moment of a function $q(E, \mu, s)$, weighted by cross-section σ is

$$\mathcal{E}_\sigma[q](t) = \int q \sigma n v f dE d\mu ds \qquad (2)$$

This equation also serves to define the expectation operator $\mathcal{E}_\sigma[]$, which in this equation represents an average of q over the distribution f weighted by cross section σ. For example, $\mathcal{E}_\sigma[q = s]/\mathcal{E}_\sigma[1]$ tells us the mean position at which the process described by σ is taking place. Note that $\mathcal{E}_\sigma[1] = I_\sigma(t)$ is the total rate of the process described by cross-section σ. The meaning of the expectation operator is most easily understood in the context of stochastic variables, discussed later in Sect. 4.

2.1. The single particle distribution

Expressions for the moments could be obtained by solving the Fokker-Planck equation and inserting the solution into (2). Alternatively, Conway et al. (1998) showed how moments can be obtained without explicit solution of the Fokker-Planck equation. However, the moments derived in that paper were for a single particle distribution. To use these results it is first necessary to show how the full distribution function can be constructed from *single particle distributions*. A single particle distribution, denoted by f_1 here, is the distribution function of a particle injected at a given instant in time, with given values of energy and pitch angle, at a given position (represented here by t_0, E_0, μ_0 and s_0 respectively). From a frequentist point of view one can also view it as the distribution function of a number of particles injected with the same initial conditions at the same time, normalised by the number of injected particles. Physically, a single particle distribution only contains information on particle transport, and contains no features from any initial distribution of particles. Mathematically, the single particle distribution $f_1(E, \mu, s; t|E_0, \mu_0, s_0)$ is defined as the distribution evolved from initial condition $f(E, \mu, s; t = 0) = \delta(E - E_0)\delta(\mu - \mu_0)\delta(s - s_0)$.

To express a general distribution f in terms of single particle distributions f_1 requires the introduction of an injection rate function $h(E_0, \mu_0, s_0; t_0)$, which is the number of particles injected per unit time at time t_0, per unit E_0, μ_0 and s_0. The general distribution f can then be formed by adding together single particle distributions, weighted by the injection function evaluated at their injection parameters (variables with subscript 0):

$$\begin{aligned} f(E, \mu, s; t) \ = \ \int & f_1(E, \mu, s; t - t_0|E_0, \mu_0, s_0) \\ & h(E_0, \mu_0, s_0; t_0) dE_0 d\mu_0 ds_0 dt_0 \end{aligned} \qquad (3)$$

It is useful to introduce the single particle expectation operator, $\mathcal{E}_1[]$ (in Conway et al. 1998 this was written 'E[]'). The single particle expectation of q is defined as

$$\mathcal{E}_1[q](t) = \int f_1 q dE d\mu ds \qquad (4)$$

This gives the expected value of q for a particle at time t that had energy E_0, pitch angle cosine μ_0 at its injection location s_0 at $t = 0$. For example, $\mathcal{E}_1[s]$ gives the expected position of the particle at time t, and $\mathcal{E}_1[s^2] - \mathcal{E}_1[s]^2$ gives the expected variance about that position. It is important to remember that because we are dealing with the single particle expectation operator, this spread in position is entirely due to transport effects, and not to any initial distribution of particles.

2.2. The time dependent case

By inserting (3) into (2), changing the order of integration, and using the definition of the single particle moments (4) we obtain

$$\begin{aligned} \mathcal{E}_\sigma[q](t) \ = \ \int & \mathcal{E}_1[q\sigma n v](t - t_0) \\ & h(E_0, \mu_0, s_0; t_0) dE_0 d\mu_0 ds_0 dt_0 \end{aligned} \qquad (5)$$

This is the important general result that underlies the subsequent theory developed in this paper. Its importance arises from the fact that observables of some process described by σ (the left hand side of (5)), such as HXR bremsstrahlung, can be directly related to moments of the injected distribution h (right hand side). The description of the particle transport is solely contained in the single particle expectation, which will be dealt with in more detail in Sect. 4.

2.3. The time independent case

To remain general to the case of an arbitrary background density distribution $n(s)$, we are forced to consider the problem as time independent, i.e. that h is independent of t_0. The fundamental reason for this will be made clear below. In order to do this a new independent variable needs to be introduced - this is path depth P. It is defined so that a particle moving at speed v, through a background of density n will encounter a path depth $dP = nvdt$ during an infinitesimal time dt. We call P "path depth" because it measures the amount of background material the particle has encountered along its path. In general, the particle will follow a helical path along a magnetic field line. Column depth, which we denote by its conventional symbol N, differs in that it is a measure of background material along a given magnetic field line (or sometimes along the vertical direction). The column depth traversed by a particle in time dt is defined as $dN = n\mu vdt$. A fundamental difference between the two is that path depth can only be discussed with reference to an energetic particle, whereas column depth can be used independently much like a distance measure, e.g. "the column depth to the transition region is N_0". We are careful to distinguish between path depth and column depth because they are easily confused, especially in 1D treatments - see MacKinnon & Brown (1989) for a discussion on this subject. The physical significance of path depth is that it measures the total amount of background material experienced by a particle up to a given point in its life. In the case of collisional interactions with background particles, the particle's energy E is a deterministic function of P, i.e. it will have a particular value for a given P, unlike pitch angle, say, which will have a distribution of values. In contrast, E and P are in general stochastic functions of t. The reasons behind this will be made clear later in Sect. 4. For now it is enough to note that because the relation between E and t is stochastic, the stopping time of a particle, which is needed as an upper limit in the time integrals, does not in general have a deterministic value. For this reason we use P rather than t as the independent variable.

Our aim is now to re-express (5) with the assumption that h is independent of t_0 and express $\mathcal{E}_1[]$ as a function of P rather than t. To achieve this, we must redefine the single particle moment to be a function of P: the function $f_1(E, \mu, s; P|E_0, \mu_0, s_0)$ is the distribution of particles with initial parameters E_0, μ_0, s_0 at $P = t = 0$, once they have traversed a path depth P. Unless the density is spatially uniform, particles injected at the same time will not all reach the same path depth P at some later time t. However, the advantage in using path depth is that in dealing with collisions with background particles, the energy distribution of f_1 is a Dirac delta function in E ($\delta(E - E(P))$). This is a mathematical statement of the fact that the energy of the particle is only dependent on the amount of background material encountered - which is exactly what is quantified by P. We can therefore write that t and P forms of f_1 are related by the following relation, for any function $r(E, \mu, s)$:

$$\int\int r(E,\mu,s) f_1(E,\mu,s;P)dEdP = \int\int r(E,\mu,s) f_1(E,\mu,s;t)n(s)v(E)dEdt \tag{6}$$

With $r = 1/nv$, this is simply equating particle number (per unit μ and s). Two cautionary notes are needed here. The above relation *does not* represent a simple change of variable, i.e.

$$f_1(E,\mu,s;P)dP \neq f_1(E,\mu,s;t)n(s)v(E)dt$$

It is the two integrals that are equal. In general, an interval of ΔP corresponds to many different time intervals because different particles with the same initial conditions will take different paths through the background media, sampling different densities as they do so. The situation is analogous to the use of a differential emission measure where a volume integral, perhaps performed over a set of concentric spherical surfaces, is replaced by an integral over surfaces of constant temperature (Craig & Brown, 1976).

To re-express (5) under the time independent assumption that h is independent of t_0, consider the time integral over the single particle expectation

$$\int \mathcal{E}_1[\sigma qnv]dt_0 = \int \sigma qnv f_1(E,\mu,s;t-t_0)dt_0 dE d\mu ds$$

Using (6) with $r = \sigma q$, we can replace the right hand side of the above equation as follows:

$$\begin{aligned} &\int \mathcal{E}_1[\sigma qnv]dt_0 \\ =& \int \sigma q f_1(E,\mu,s;P)dEdPd\mu ds \\ =& \int \mathcal{E}_1[\sigma q]dP \end{aligned}$$

It is now clear, at least mathematically, why an arbitrary density distribution necessitates a time-independent treatment. The entire mathematical argument, from (6) onwards, is predicated on the assumption that h can be removed from the t_0 integral. If this were not the case, then the presence of t_0 in h presents an insurmountable problem because we are *not* simply making a change of variables from t_0 to P. Physically, it is not meaningful to write the injection rate h as a function of P, because P is defined in relation to the evolution of a particle, and cannot be related directly to an external independent variable such as time t_0. The fundamental reason for this problem is that we made a prior assumption that P and E are deterministically related. This assumption was made because all currently known solutions to the single particle moments have this property. In fact the deterministic relation of E and P is guaranteed for any process affecting particle energy, that has a cross-section proportional to nv.

The time independent, arbitrary background density version of (5) is therefore

$$\mathcal{E}_\sigma[q] = \int \mathcal{E}_1[q\sigma](P)dPh(E_0,\mu_0,N_0)dE_0 d\mu_0 dN_0 \tag{7}$$

To be completely general to any distribution of density, the column depth N_0 is used in the above equation in place of s_0. This is a straightforward change of variable that requires a model for $n(s)$ if N and s are to be related.

3. Specific cross-sections

3.1. Hard X-ray (HXR) moments

Energetic electrons moving through a plasma will experience close (relative to the collisions dominating their energy loss and scattering) collisions with protons and ions that result in the emission of HXR bremsstrahlung radiation. This is described by the well known Bethe-Heitler cross-section $\sigma(E,\epsilon)$, which has mathematical form:

$$\sigma_X(E,\epsilon) = \frac{\sigma_0}{E\epsilon} H(E-\epsilon)\log\frac{1+(1-\epsilon/E)^{1/2}}{1-(1-\epsilon/E)^{1/2}} = \frac{\sigma_0}{E\epsilon} L(E,\epsilon) \quad (8)$$

where ϵ represents the emitted photon energy, $\sigma_0 = 7.9 \times 10^{-29}\mathrm{m}^2$ keV, and $H(x)$, the Heaviside step function, is 1 for $x > 0$ and zero otherwise. Note that L and σ_X are defined to be zero when the electron energy E is less than the photon energy ϵ. This allows us to keep the limits of the energy integrals in the moments as 0 and ∞.

Consider the single particle expectation $\mathcal{E}_1[q\sigma]$, where q is some function of E, μ, s that is of interest. $\mathcal{E}_1[\sigma nv]$ is the HXR emission rate due to a single particle, per unit photon energy. The quantity $\mathcal{E}_1[q\sigma nv]/\mathcal{E}_1[\sigma nv]$ therefore represents an averaging of q over the emission of a single particle. More generally, we can define the average over the whole electron distribution f, using the the expectation operator $\mathcal{E}_X[]$ defined by (5) or (7) with σ_X given by (8):

$$\langle q\rangle_\mathrm{X} = \frac{\mathcal{E}_\mathrm{X}[q]}{\mathcal{E}_\mathrm{X}[1]} \quad (9)$$

This equation can be used to relate an observable (left hand side), such as the centroid of the HXR emission at a particular photon energy $\langle s\rangle_\mathrm{X}$, to terms on the right hand side that will involve moments of the injected distribution h, such as the mean injected pitch angle or the mean injected position. Referring to equation (1), the quantity $I_X(t) = \mathcal{E}_X[1]$ is the rate of HXR photon emission at energy ϵ, per unit ϵ, at time t, from the whole electron distribution described by f.

3.2. Heating moments

Heating moments are very similar in form to the HXR moments, and are in fact simpler because there is no introduction of a further variable, such as the photon energy ϵ. The cross-section is given by

$$\sigma_H = \frac{C}{E} \quad (10)$$

where $C = 2\pi e^2\Lambda$ and e is the electronic charge (in e.s.u.) and Λ is the Coulomb logarithm, which we assume to be constant. Despite the $1/E$ dependence and the lower limit of the energy integrals in the moments being $E = 0$, the integrals do not diverge because of the presence of nv in the integrands.

4. Derivation of moment expressions

Application of the above theory requires information on the single particle distribution function f_1, that describes the propagation of a single injected particle. More precisely, moments of f are needed. These have been calculated analytically by Conway et al. (1998) for the case of non-relativistic electrons in a constant magnetic field f_1. Here we develop the use of the preceding theory by using those results.

4.1. Stochastic variables and single particle moments

A single particle distribution function, $f_1(E, \mu, s; t|E_0, \mu_0, s_0, t_0)$, describes the distribution associated with a single particle, that was injected at time t_0, with energy E_0, pitch angle cosine μ_0 at position s_0. We will consider the case where the background density distribution is arbitrary but the magnetic field strength is constant. For this case, MacKinnon & Craig (1991) showed that the Fokker-Planck equation is equivalent to 3 coupled Stochastic Differential Equations (SDEs), also known as Îto equations:

$$\begin{aligned} d\hat{s} &= \hat{\mu}v(\hat{E})dt \\ d\hat{E} &= -\frac{Cn(\hat{s})v(\hat{E})}{\hat{E}}dt \\ d\hat{\mu} &= -\frac{Cn(\hat{s})v(\hat{E})\hat{\mu}}{\hat{E}^2}dt \\ &\quad + \left[\frac{Cn(\hat{s})v(\hat{E})(1-\hat{\mu}^2)}{2\hat{E}^2}\right]^{1/2} d\hat{W}(t) \end{aligned}$$

where $C = 2\pi e^4\Lambda$. These express the progress of a particle as a series of increments in each of the dependent variables: $\hat{s}$, $\hat{E}$ and $\hat{\mu}$ (or z, v and μ in MacKinnon & Craig 1991). The hat symbol is used to emphasise that these variables are *stochastic variables*. Stochastic variables do not necessarily have a given value at a given time; they have a distribution of possible values that is described by the single particle distribution f_1. Each equation contains a dt term; this represents a conventional deterministic change in that variable with the independent variable t. The $d\hat{\mu}$ equation also contains a $d\hat{W}(t)$ term; this term represents a stochastic change in $\hat{\mu}$ in an infinitesimal time step dt. $d\hat{W}(t)$ is known as a Wiener process, which formally is a (Dirac) delta-correlated white noise time series. It can be defined in a number of other ways. For example, it can be considered as the limit of a discrete white noise time series of time-step Δt, as $\Delta t \to dt$. Integration of $d\hat{W}(t)$ from 0 to time t gives $\hat{W}(t)$, which is a white noise, normally (Gaussian) distributed stochastic variable with mean 0 and variance $2t$. To clarify the meaning of $d\hat{W}(t)$, it is helpful to consider how it would be implemented in a numerical code. Let the code's time-step be Δt, and let $-g(\hat{E})\hat{\mu}$ be the coefficient of dt in the $d\hat{\mu}$ equation. The $d\hat{\mu}$ equation is implemented by adding $-g(\hat{E})\hat{\mu}\Delta t$ to the previous $\hat{\mu}$ value, *plus* a zero-mean, variance 2, Gaussian distributed random number multiplied by $\sqrt{g(\hat{E})(1-\hat{\mu})/2}$. (Note the convention of the Wiener process having a variance of 2, rather than 1).

The presence of the Wiener process is only explicit in the $d\hat{\mu}$ equation, though $\hat{\mu}$ appears in the $d\hat{s}$ equation, making $\hat{s}$ a stochastic variable also. If the density n is not spatially uniform, then the density at the particle's position $\hat{s}$ will become a stochastic quantity. This means that, in general, $\hat{E}$ is also a stochastic variable. If the density is uniform however, then the $\hat{E}$ equation becomes deterministic and can be integrated to give an explicit function of time. This is a tremendous simplification, as it makes the system of equations (nearly) linear, and thus easily soluble. The same simplification can be made for the non-uniform density if the path depth P is used as the independent variable instead of t. The cost is of course that the time dependence is no longer explicit. Changing from t to P yields the following set of equations:

$$\begin{aligned} d\hat{N} &= \hat{\mu} dP \\ d\hat{E} &= -\frac{C}{\hat{E}} dP \\ d\hat{\mu} &= -\frac{C\hat{\mu}}{\hat{E}^2} dP + \left[\frac{C(1-\hat{\mu}^2)}{2\hat{E}^2}\right]^{1/2} d\hat{W}(P) \end{aligned}$$

where $d\hat{N} = n(\hat{s})d\hat{s}$ and $d\hat{P} = n(\hat{s})v(\hat{E})dt$. The middle equation can be integrated straightforwardly, allowing the appearances of $\hat{E}$ in the first and second equations to be substituted with an explicit function of P. This means that these equations are essentially linear in nature (despite the appearance of $1-\hat{\mu}^2$ in the stochastic term). The correspondence of the notation of Conway et al. (1998) to the present notation (the right hand sides) is as follows: $y = \hat{N}/P_S(E_0)$, $x = P/P_S(E_0)$, where $N_s(E_0) = P_S(E_0)$ is the path depth (integrated along a particle's path) required to stop a particle of initial energy E_0.

It is clear that $\hat{E}$ is a deterministic function of P. In other words, it has a mean that is a function of P and always has zero variance. The physical reason for this deterministic relationship is that the energy of the fast particle is assumed to be much greater than the thermal energies of the background particles. As a result it is pulled inexorably back into the background distribution. Once a particle's energy nears the thermal energy, neglected terms in the fast particle Fokker-Planck equation will become important, and this treatment will no longer be appropriate. Contrast this with situation when the μ distribution is far from being isotropic, e.g. for a directed beam with $\mu = 1$ (zero pitch angle). As can be seen from the $d\hat{\mu}$ equation in (11), the stochastic term vanishes for this case, and the deterministic term pulls $\hat{\mu}$ to lower values. As this happens, the stochastic term grows, and by the stopping time, $\hat{\mu}$ will in fact b be distributed uniformly, i.e. the particle velocity will have an isotropic distribution.

Now that stochastic variables have been introduced, it is much easier to interpret the meaning of the expectation operator. For example, $\mathcal{E}_1[\hat{\mu}](t)$ is the expected pitch angle cosine for a particle with given injection parameters (E_0, μ_0, s_0) at a time t after its injection. Similarly, $\mathcal{E}_1[\hat{s}](t)$ is the particle's expected location. The spread about this position is measured by $\sqrt{\mathcal{E}_1[\hat{s}^2](t) - \mathcal{E}_1[\hat{s}]^2(t)}$. Similar expressions can be used when working with path depth P as the independent variable. The moments denoted by $\mathcal{E}_\sigma[]$ represent averages over the transports effects, together with the initial distribution, weighted according to the cross-section of interest σ.

4.2. Time independent: arbitrary density

The results below apply to the case of continuous steady injection of a distribution of electrons. So as to remain general to any density distribution, we will work with column depth $N = \int n ds$ (i.e. density integrated along the magnetic field). We wish to answer the following questions: 1) Where is the centroid of the HXR emission? 2) What is the apparent size of the HXR source? 3) Where is the electron distribution's energy mainly deposited? 4) What is the extent of this energy deposition region? We will answer the first two questions in detail, but just state the results for the last two, as the calculations involved are very similar.

Before proceeding, we quote the main results of Conway et al. (1998) in the notation of this paper, adding terms that generalise those results, which assumed injection at $N = 0$, to have injection at $N = N_0$:

$$\mathcal{E}_1[\mu] = \mu_0 x \tag{11}$$

$$\mathcal{E}_1[\mu^2] = \left(\mu_0^2 - \frac{1}{3}\right) x^3 + \frac{1}{3} \tag{12}$$

$$\mathcal{E}_1[N] = N_0 + \frac{2}{3}\mu_0 P_S \left(1 - x^3\right) \tag{13}$$

$$\begin{aligned} \mathcal{E}_1[N^2] &= N_0^2 + \frac{4}{3}\mu_0 P_S N_0 \left(1 - x^3\right) \\ &\quad + \frac{2}{21} P_S^2 \left(4\mu_0^2 + 1 + (3\mu_0^2 - 1)x^7 + 7x^4 \right. \\ &\quad \left. - 7\left(\mu_0^2 + 1\right) x^3\right) \end{aligned} \tag{14}$$

where $x = E/E_0$ and the stopping path depth is $P_S = E_0^2/2C$. It is interesting to note that the final ($x = 0$) spread of the electrons' positions in terms of column depth N is given by

$$\sqrt{\mathcal{E}_1[N^2] - \mathcal{E}_1^2[N]} = \left[\frac{2}{21}\left(1 - \frac{2}{3}\mu_0^2\right)\right]^{1/2} P_S$$

So for a completely directed, zero pitch angle ($\mu_0 = 1$) monoenergetic beam, this spread will be $0.178 P_S$, which is about a quarter of the stopping depth in terms of $\mathcal{E}_1[N] = 0.667 P_S$. For a distribution with only $90°$ pitch angles initially ($\mu_0 = 0$), the final spread is $0.309 P_S$. Note that in using such expressions to make rough estimates of HXR source sizes or positions at photon energy ϵ, $x = \epsilon/E_0$ should be used instead of $x = 0$. This leads to smaller values for such quantities.

Inserting the above expressions into (7), changing variable from path depth P to energy $E = E_0(1 - P/P_S)^{1/2}$ and using the Bethe-Heitler cross-section (8) will result in having to deal with integrals of the form

$$\begin{aligned} q_{lmnp} &= \frac{\sigma_0}{C\epsilon} \int\int\int_{E_L}^{E_U}\int_{\epsilon}^{E_0} L(E,\epsilon)\mu_0^l E_0^m x^n N_0^p dE \\ &\quad h(E_0, \mu_0, N_0) dE_0 d\mu_0 dN_0 \end{aligned}$$

$$= \frac{\sigma_0}{C\epsilon}\int\int\int_{\epsilon}^{E_U} L(E,\epsilon)E^n \int_{\max[E,E_L]}^{E_U} \mu_0^l E_0^{m-n} h(E_0,\mu_0,N_0)dE_0 d\mu_0 dN_0 dE \quad (15)$$

where l, m, n are integers. The second integral, which is more convenient to evaluate, is obtained by reversing the order of integration of E and E_0. Explicit higher and lower energy limits, E_U and E_L respectively, are placed on the injected distribution function here because we will see later that the spatial HXR variance can become infinite if electrons of infinite energy are present. The practical justification for assuming upper and lower cutoffs is discussed in Sect. 4.3. To proceed from here requires assumptions to be made about the form of h. We will assume that the distribution is a power law, and that it is separable in (N_0, μ_0) and E_0, i.e. it can be written as follows $\int h\mu_0^l N_0^p d\mu_0 dN_0 = \langle \mu_0^l N_0^p\rangle H_0 E_0^{-\delta}$. Here $\delta = \delta_F + 1/2$, where δ_F is commonly used electron flux power law index. H_0 is defined so that the total number of electrons injected per unit time is given by

$$R = \frac{H_0}{\delta - 1}\left(E_L^{1-\delta} - E_U^{1-\delta}\right)$$

Evaluating the E_0 integral of (15) yields

$$q_{lmnp} = \frac{\sigma_0 H_0}{C\epsilon k}\langle \mu_0^l N_0^p\rangle \int_{\epsilon}^{E_U} L(E,\epsilon) E^n\left(\max[E,E_L]^{-k} - E_U^{-k}\right)dE$$

where $k = \delta + n - m - 1$. By splitting the integral at $E = E_L$, it can be evaluated to

$$q_{lmnp} = \frac{\sigma_0 H_0}{C\epsilon k}\langle \mu_0^l N_0^p\rangle \left(\frac{\epsilon^{-j}}{j} B_{\xi_H,\xi_L}\left(j,\frac{1}{2}\right) + \left[\frac{E^{-j}L(E,\epsilon)}{n+1} - \frac{\epsilon^{n+1}}{n+1}E^{-k} B_{\xi,1}\left(-(n+1),\frac{1}{2}\right) - \frac{E^{-j}L(E,\epsilon)}{j}\right]_{E_L}^{E_U}\right) \quad (16)$$

where $j = \delta - m - 2$ and $\xi = \epsilon/E$. The function $B_{x,y}(a,b)$ is the same as the standard Beta function, except that its limits are replaced by x and y:

$$B_{x,y}(a,b) = \int_x^y z^{a-1}(1-z)^{b-1}dz$$

At this point we can make two simplifying assumptions, which are commonly made elsewhere in HXR bremsstrahlung calculations: $E_U \to \infty$ and the photon energy of interest is higher than the lower cutoff of the injected distribution, this means we can replace all occurrences of E_L with ϵ. This results in a much simpler expression:

$$q_{lmnp} = \frac{\sigma_0 H_0 \langle N_0^p \mu_0^l\rangle B(j,\frac{1}{2})}{Cjk}\epsilon^{-j-1} \quad (17)$$

Notice that $q_{0000} = \mathcal{E}_X[1]$ is simply the HXR thick target expression.

We are now in a position to calculate the desired moments. Firstly, from (11) we can write that, for $\delta > 2$:

$$\mathcal{E}_X[\mu] = q_{1010} = \frac{\sigma_0 H_0\langle\mu_0\rangle}{C(\delta-2)\delta}B\left(\delta-2,\frac{1}{2}\right)\epsilon^{1-\delta}$$

Therefore, the average pitch angle of the electrons emitting HXRs is simply:

$$\langle\mu\rangle_X = \frac{\mathcal{E}_X[\mu]}{\mathcal{E}_X[1]} = \frac{\delta-1}{\delta}\langle\mu_0\rangle$$

which is actually independent of the photon energy ϵ. $\langle\mu_0\rangle$ is the average pitch angle of the injected distribution.

To calculate the spread of pitch angles, we need to calculate $\langle\mu^2\rangle_X$, which for $\delta > 2$ is given by

$$\langle\mu^2\rangle_X = \frac{\mathcal{E}_X[\mu^2]}{\mathcal{E}_X[1]} = q_{2030} - \frac{1}{3}q_{0030} + \frac{1}{3}q_{0000} = \frac{1 + (\delta-1)\langle\mu_0^2\rangle}{\delta+2}$$

In a similar fashion, the following two column depth moments can be shown to be:

$$\langle N\rangle_X = \langle N_0\rangle + \langle\mu_0\rangle P_S(\epsilon)g_1(\delta) \quad (18)$$

$$\langle N^2\rangle_X = \langle N_0^2\rangle + 2\langle\mu_0 N_0\rangle P_S(\epsilon)g_1(\delta) + \left(1 + \langle\mu_0^2\rangle(\delta-1)\right)P_S^2(\epsilon)g_2(\delta) \quad (19)$$

where

$$g_1(\delta) = 2\frac{(\delta-\frac{3}{2})(\delta-\frac{5}{2})(\delta-1)}{\delta(\delta-3)^2(\delta-4)}$$

$$g_2(\delta) = 8\frac{(\delta-\frac{3}{2})(\delta-\frac{5}{2})(\delta-\frac{7}{2})(\delta-\frac{9}{2})}{(\delta+2)(\delta-2)(\delta-3)(\delta-4)(\delta-5)^2(\delta-6)}$$

Note that $\langle N\rangle_X$ remains finite only for $\delta > 4$, and $\langle N^2\rangle_X$ for $\delta > 6$. The appearance of a factor $\delta - n$ in a denominator does not necessarily mean that a moment is undefined at $\delta = n$, though the above expressions *are* undefined. Careful consideration of the integration in these cases can yield well-behaved mathematical expressions.

Assuming an upper cut-off, for whatever reason, can lead to counter-intuitive results, especially in light of the usual situation where it is assumed that only a lower cutoff is important. One surprise is that the size of a HXR source does not simply scale as $P_S(\epsilon) = \epsilon^2/2C$. This is illustrated in Fig. 1 for an isotropic source, for a range of photon energies, and for three upper cut-off values, $E_U = 40$ keV, $E_U = 70$ keV and $E_U = 100$ keV.. The departure from ϵ^2 scaling is most pronounced for low values of δ. The tangent of these curves only accords with a line of gradient ϵ^2 for large δ and $\epsilon \ll E_U$. When ϵ becomes a sizeable fraction of E_U, the source size can even decrease with photon energy. This behaviour was observed for the 13th Jan. 1992 (Masuda) flare (Masuda et al. 1995), which had a hard (low δ)

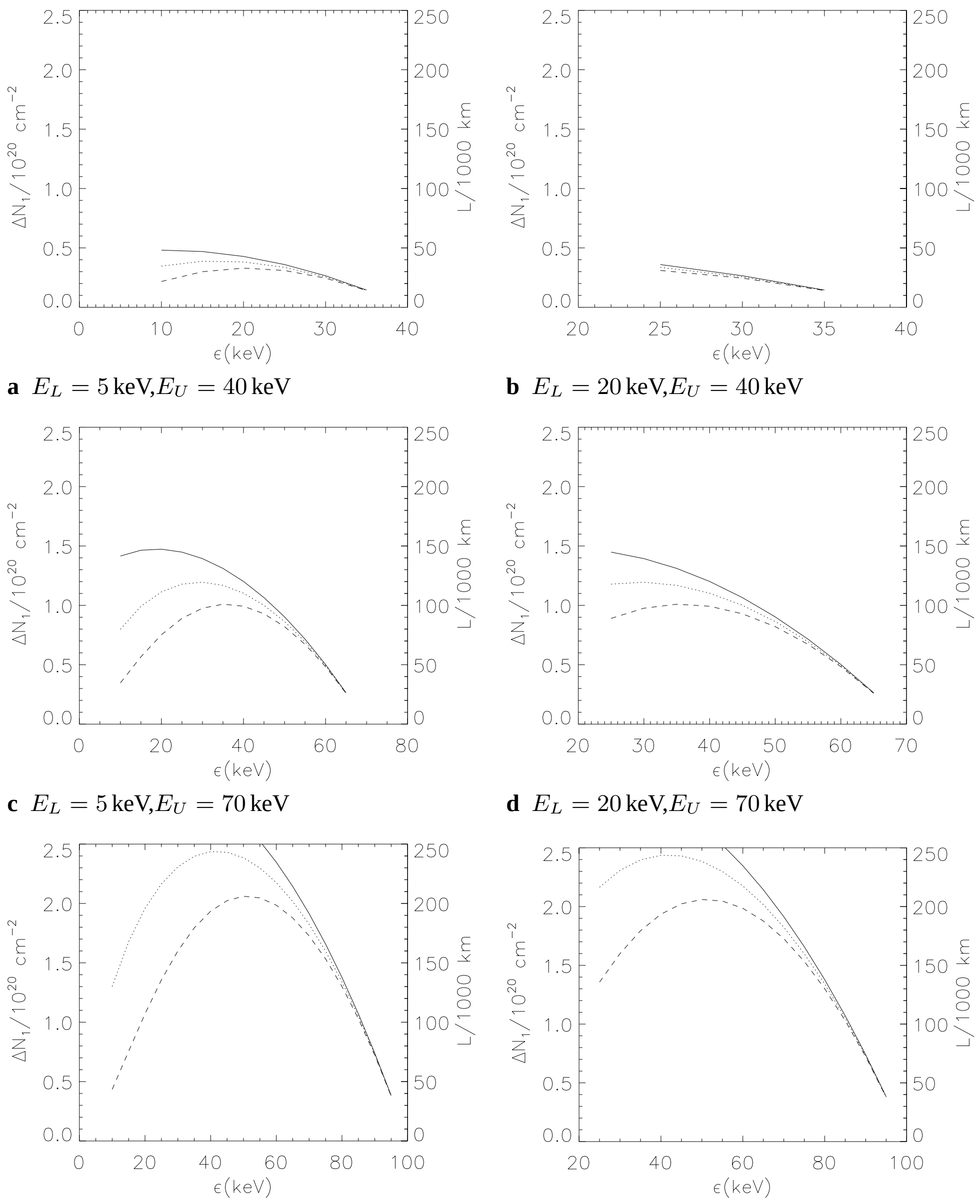

a $E_L = 5\,\mathrm{keV}, E_U = 40\,\mathrm{keV}$ **b** $E_L = 20\,\mathrm{keV}, E_U = 40\,\mathrm{keV}$

c $E_L = 5\,\mathrm{keV}, E_U = 70\,\mathrm{keV}$ **d** $E_L = 20\,\mathrm{keV}, E_U = 70\,\mathrm{keV}$

e $E_L = 5\,\mathrm{keV}, E_U = 100\,\mathrm{keV}$ **f** $E_L = 20\,\mathrm{keV}, E_U = 100\,\mathrm{keV}$

Fig. 1a–f. Plots of the apparent size of a HXR source in terms of: column depth, i.e. $\Delta N = \sqrt{\langle N^2 \rangle_X}$; and $L = \Delta N/n$, the spatial extent along a loop of constant density $n = 10^{10}\,\mathrm{cm}^{-3}$. For the largest ΔN values, L is unrealistically large, which can be interpreted as E_U being too large. Curves for three different δ values are shown on each plot: $\delta = 2$ is the upper (solid) curve, $\delta = 4$ is middle (dotted) curve and $\delta = 6$ is the lowest (dashed) curve. The injected distribution is isotropic, i.e. $\langle \mu_0 \rangle = 0$ and $\langle \mu_0^2 \rangle = 1/3$.

spectrum. There are two explanations for this counter-intuitive effect. One is simply that for ϵ close to E_U, only the highest energy electrons contribute, and do so only for a short time, during which they cannot move too far. Secondly, the relatively long collisional time for these higher energy electron means that those with large pitch angle electrons will take longer to diffuse away from their starting position than electrons with lower energy. This can be seen from the expression derived for 'τ_L' in Conway et al. (1998).

The *heating moments* are easier to calculate and the relevant expressions for μ N, where $\langle q \rangle_h = \mathcal{E}_H[q]/\mathcal{E}_H[1]$, are

$$\langle \mu \rangle_H = \frac{\langle \mu_0 \rangle}{2} \tag{20}$$

$$\langle \mu^2 \rangle_H = \frac{\langle \mu_0^2 \rangle + 1}{4} \tag{21}$$

$$\langle N \rangle_H = \langle N_0 \rangle + \frac{\langle \mu_0 \rangle}{4C} \frac{\delta - 2}{\delta - 4} \frac{E_L^{4-\delta} - E_U^{4-\delta}}{E_L^{2-\delta} - E_U^{2-\delta}} \tag{22}$$

$$\langle N^2 \rangle_H = \langle N_0^2 \rangle + \frac{\langle \mu_0 N_0 \rangle}{2C} \frac{\delta - 2}{\delta - 4} \frac{E_L^{4-\delta} - E_U^{4-\delta}}{E_L^{2-\delta} - E_U^{2-\delta}} + \frac{5 \langle \mu_0^2 \rangle + 1}{80C^2} \frac{\delta - 2}{\delta - 6} \frac{E_L^{6-\delta} - E_U^{6-\delta}}{E_L^{2-\delta} - E_U^{2-\delta}} \tag{23}$$

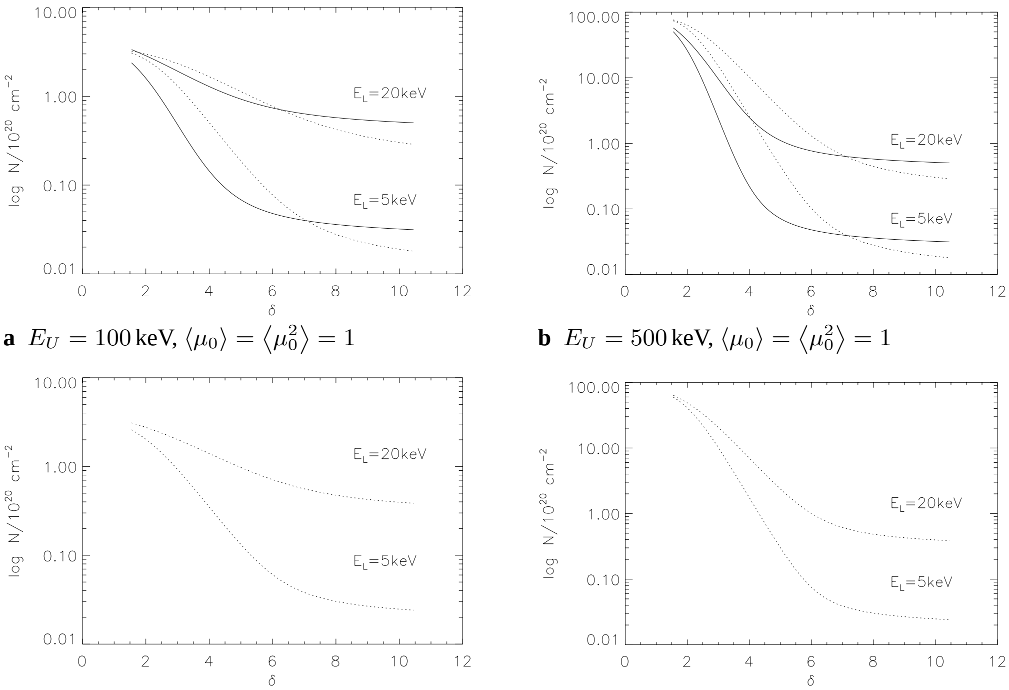

a $E_U = 100\,\text{keV}$, $\langle\mu_0\rangle = \langle\mu_0^2\rangle = 1$

b $E_U = 500\,\text{keV}$, $\langle\mu_0\rangle = \langle\mu_0^2\rangle = 1$

c $E_U = 100\,\text{keV}$, $\langle\mu_0\rangle = 0, \langle\mu_0^2\rangle = 1/3$ (isotropic)

d $E_U = 500\,\text{keV}$, $\langle\mu_0\rangle = 0, \langle\mu_0^2\rangle = 1/3$ (isotropic)

Fig. 2a–d. Plots of the mean column depth of energy deposition (solid) and the standard deviation (dashed) for a variety of parameters.

It is interesting to note that the pitch angle moments are independent of the electron energy spectrum. In contrast, the column depth moments can be very sensitive to assumptions made about the electron spectrum, especially the upper cutoff E_U. In general, this will correspond to a real cutoff in the electron distribution. However, in certain applications an effective upper cutoff may be appropriate, as previously discussed in relation to HXR moments. For example, in computing the Hα impact polarisation due to a particle beam, knowledge of pitch angle moments is needed in a restricted range of depths for particular electron energies (Henoux & Vogt 1998).

Plots of the average column depth of heat deposition $\langle N\rangle_H$ and the spread of depths $\sqrt{\langle N^2\rangle_H - \langle N\rangle_H^2}$ are shown for selected values of E_L, E_U, $\langle\mu_0\rangle$ and $\langle\mu_0^2\rangle$, in Figs. 2a, 2b and 2c.

The sensitivity of spatial moments to high energy features in the spectrum, and also their insensitivity to the lower cut-off, could lead to new diagnostics of otherwise unobservably high energy electrons. To achieve this, calibration of the relationships is needed from observations where both the spatial and spectral information is available. Also, any effective upper cut-off, as discussed above, must be carefully considered in applying the results in this way.

4.3. Cutoffs

It is clear that cutoffs in the electron spectrum have to be assumed to avoid unphysically infinite moments. We now discuss what determines these cutoffs in practice, giving particular attention to the upper cutoff because it will often be the most problematic in applying the present theory. It is important to realise that the value of the upper cutoff, E_U, need not arise from basic physics alone, but can often depend on how moments are deduced from the observations. As such, the relevance of the considerations discussed below can vary from application to application. Another point to note is that a literal cut-off is not necessarily required, a more gradual roll-over, or a break to a different spectral index can serve the same purpose.

The most obvious justification for assuming a cutoff in the electron spectrum is if there is evidence for one in the observed HXR photon spectrum. However, lower cutoffs are usually masked by thermal emission and upper cutoffs are only rarely observed. An upper cutoff at a few tens of MeV was reported by Trottet et al. (1998) for the flare of 11 June 1990. In general, E_L will probably be less than 20 keV and E_U will be greater 1 MeV; though more restrictive limits will be possible for some large flares. Depending on the value of δ, and the moment in question, one or other of these cutoffs may dominate the moment expressions, and the other may be set to its extreme value (i.e. zero or infinity).

In many cases of interest, an effective cutoff can be more important than any real cutoff in the electron spectrum. For example, an upper cutoff of 10 MeV in the electron spectrum cannot possibly be relevant in determining the apparent size of a coronal HXR (say 10–100 keV) source. This is because electrons at energies of a few MeV will contribute much less to this emission than electrons at energies of a few tens of keV. The effective upper cutoff in this case would depend on both the observed photon energy range and the energy corresponding to the column depth of the coronal material. Similarly in applying the results to Hα impact polarisation, only electrons in certain ranges of energy and depth are relevant, thus introducing effective lower and upper cutoffs.

4.4. Time dependent: constant density

The time dependent case can only be considered if the density is uniform in space, because then the path depth P is a deterministic function of time t:

$$P(t) = P_S\left(1-\left(1-\frac{t}{\tau}\right)^{4/3}\right)$$

$$\tau = \frac{4P_S}{3nv_0} = \frac{\sqrt{2m}E_0^{3/2}}{3Cn} \tag{24}$$

where τ is the stopping time. For the same reason, N and s are simply related to each other: $N = ns$. Given the extra freedom of choosing how the injection function h varies with time, specific results can only be obtained by making further assumptions. Here we are only concerned with calculating $\langle t\rangle_X$ and $\left\langle t^2\right\rangle_X$, which tells us the time, and the time interval, during which the HXR emission at a particular photon energy ϵ will take place. These times are defined in relation to the moments $\langle t_0\rangle$ and $\left\langle t_0^2\right\rangle$, which are obtained by integrating $h(E_0,\mu_0,s_0;t_0)$ multiplied by t_0 and t_0^2 respectively, over all E_0,μ_0,s_0 and also t_0. Although it is possible to calculate the time-dependent moments of μ and s (E is deterministic in time here), as defined in (5), doing so requires more information than the first two temporal moments of h provide. Further assumptions must be made relating to specific circumstances in order to give useful results, so we will not consider this case in this paper.

Firstly, the temporal moments of the HXR intensity distribution, T_i are defined:

$$T_i = \int \mathcal{E}_X[1](t)t^i dt \tag{25}$$

remembering that $\mathcal{E}_X[1](t)$ is the HXR intensity as discussed in Sect. 2. It is therefore clear that the normalised moments in time are given by: $\langle t\rangle = T_1/T_0$ and $\left\langle t^2\right\rangle = T_2/T_1$.

Using (5) to expand (25) with the Bethe-Heitler cross-section given by (8) will result in time integrals (in t) of the form:

$$\int t^i \frac{vL(E,\epsilon)}{E}dt$$

where E (and therefore $v(E)$) is a function of $t-t_0$. Changing variable to E using the relation

$$E = E_0\left(1-\frac{t-t_0}{\tau(E_0)}\right)^{2/3}$$

gives the integral in the following form:

$$\frac{\sigma_0}{C\epsilon}\int\left[t_0+\tau(E_0)\left(1-\left(\frac{E}{E_0}\right)^{3/2}\right)\right]^i L(E,\epsilon)dE$$

This integral must also be integrated over E_0,μ_0,s_0 and t_0. The integration over E_0 can be written in terms of q_{lmnp} introduced in (15). Doing so gives:

$$T_0 = q_{0000} \tag{26}$$

$$T_1 = \langle t_0\rangle q_{0000} + \frac{\sqrt{2m}}{3Cn}\left[q_{0\frac{3}{2}0} - q_{0\frac{3}{2}\frac{3}{2}}\right] \tag{27}$$

$$T_2 = \left\langle t_0^2\right\rangle + 2\langle t_0\rangle\frac{\sqrt{2m}}{3Cn}\left[q_{0\frac{3}{2}0} - q_{0\frac{3}{2}\frac{3}{2}}\right] + \frac{2m}{(3Cn)^2}\left[q_{030} - 2q_{03\frac{3}{2}} + q_{033}\right] \tag{28}$$

The integral over t_0 simply means replacing instances of t_0^n with $\langle t_0^n\rangle$. Doing this assuming that $h = H_0(\mu_0,s_0;t_0)E_0^{-\delta}$ and using the expression for q in (17), gives the final results:

$$\langle t\rangle_X = \langle t_0\rangle + u_1(\delta)\tau(\epsilon) \tag{29}$$

$$\left\langle t^2\right\rangle_X = \left\langle t_0^2\right\rangle + 2u_1(\delta)\tau(\epsilon)\langle t_0\rangle + u_2(\delta)\tau(\epsilon)^2 \tag{30}$$

where

$$u_1(\delta) = \frac{3(\delta-2)B(\delta-\frac{7}{2},\frac{1}{2})}{2(\delta-\frac{5}{2})(\delta-\frac{7}{2})B(\delta-2,\frac{1}{2})}$$

$$u_2(\delta) = \frac{9(\delta-2)B(\delta-5,\frac{1}{2})}{2(\delta-\frac{5}{2})(\delta-4)(\delta-5)B(\delta-2,\frac{1}{2})}$$

This result is valid for $\delta > 5$. A more general expression can be calculated using the general expression for q in (16). Note also that the form used for h above assumes that the distribution is separable in E_0 and t_0 - i.e. the injection spectrum is time-independent. The time delay between the HXR flux's peak at photon energy ϵ and the peak in the rate of electron injection is simply $\langle t\rangle - \langle t_0\rangle$. This is clearly proportional to $\tau(\epsilon)$ which itself is proportional to $\epsilon^{3/2}$. Numerical evaluation of the factor involving δ show that it decreases with δ. This is expected as larger δ means relatively more low energy electrons, and so shorter electron life-times. The same conclusions can be made for the width of the HXR peak of emission, $\sqrt{\langle t^2\rangle - \langle t\rangle^2}$. Note that all of these conclusions can be radically changed, and become much less intuitive, when δ approaches 5 and the upper cut-off (or break in the power law) is not much larger than ϵ.

5. Discussion

The results presented in this paper allow observables, such as the location and extent of a spatially resolved HXR source, to be simply related to moments of the original distribution. The zeroth order HXR moment is in fact the thick target bremsstrahlung integral. In this sense, the theory presented here is a generalisation of the results of Brown (1971). The key result of this paper can be summarised as follows: A potentially observable moment $\langle q\rangle_\sigma$, where σ corresponds to either HXRs (X) or heating (H), can be expressed as simple function of the moments of the injected particle distribution $\langle q_0\rangle$

An important issue when using moments is the effect of any lower or upper cutoff (or breaks) in the electron spectrum. For harder spectra (smaller spectral indices), moments can be very sensitive to them, and can even become infinite, even when the HXR emission is finite. These problems are mathematical, and are due to infinite energy limits in the integrals. In reality, there must be an upper cutoff, but in practice effective cut-offs will be introduced according to how the moment is measured in the observations. It would be interesting to exploit this cut-off sensitivity to devise a method of identifying spectral features at unobservably high energies. For example, if the depth range of particle beam heating can be estimated in a flare, and the spectral index of the particle distribution is also known, it would be possible to estimate the upper cutoff E_U.

The spatial HXR moments are probably of most immediate interest. If the location and size of a HXR source can be measured in a particular flare, this can be compared with $\langle N \rangle_X$ and $\sqrt{\langle N^2 \rangle_X - \langle N \rangle_X^2}$. Such a comparison requires an assumption about the density structure. For spatially resolved HXR emission in the corona, such as the HXR above the loop top sources (Masuda 1994, Masuda et al. 1995), a density structure along the loop must be assumed. If a constant density is supposed, then the conversion of column depth to length is straightforward. However, potential complications arise if high density pockets exist as was proposed as an explanation for the HXR coronal source by Wheatland & Melrose (1995). In such a case an average density might be assumed. If a model is assumed for how the density varies through the transition region and into the chromosphere, then statements can be made about the expected footpoint brightness. For example, if it is supposed that the energy is released at the loop-top, then one would expect relatively bright footpoints if $\sqrt{\langle N^2 \rangle_X - \langle N \rangle_X^2} \gg N_C$, where N_C is the column depth from the loop-top to the transition region.

Without further knowledge of the distribution, it is not possible to make precise theoretical statements such as: "68% of the emission lies within one standard deviation of the centroid". However, the reality is that making such definite statements from current observations is not possible, for several reasons. Even the best observed example of a coronal HXR source to date was subject to observational limitations leading to debate about its detailed characteristics (Alexander & Metcalf 1997). This is partly due to the fact that HXR coronal sources are weak, and partly due to the characteristics of the instrument and how the image is constructed. Instruments such as the Yohkoh Hard X-ray Telescope (HXT), and the High Energy Solar Spectroscopic Imager (HESSI) rely on images being reconstructed by the Maximum Entropy Method (or some similar method) to yield an image that both matches the observed data and satisfies some further regularisation constraint. This latter constraint is required to make up for "missing information", and is usually taken to be that the image is the smoothest one that fits the observations. Clearly, the detailed structure of HXR sources will be affected by this smoothing constraint in a way that is difficult to quantify. This means that it is not possible at present to make a detailed comparison between theory and observation. For example, it is not realistic make deduction concerning the electron distribution from the shape of a HXR source. Estimating the observational effects on the broad properties of the distribution (i.e. moments) is therefore a more realistic proposition.

Given the observed location and extent of the HXR source, it is possible to estimate moments of the injected distribution using the expressions derived in Sect. 4.2. Specifically, the observed location and extent of a HXR source are simply related to the location and extent of the injection region, and the average injected pitch angle and the spread in injected pitch angle. That is, the first two moments of the HXR spatial distribution give information on the first two spatial and pitch angle moments of the injected electron distribution. Clearly, four quantities of interest cannot be extracted from two observables. Either assumptions must be made, or, preferably, other observations must be used. One possibility is to try and estimate the pitch angle moments using the expressions given for $\langle \mu \rangle_X$ or $\langle \mu^2 \rangle_X$. These are averages weighted in terms of the number of electrons that are emitting HXRs at a given photon energy ϵ. In particular, $\langle \mu \rangle_X$ is very simply related to the average pitch angle of the injected distribution, and for larger δ values becomes nearly equal to it. Information on these can be obtained from directional or polarimetric properties of the HXRs. At present, methods for observing these properties in a single flare do not exist. The possibility of gaining such information about the injected distribution provides motivation for making stereoscopic and polarimetric HXR observations in the future. Another possibility might be to deduce pitch angle moments from observations of Hα impact polarisation (Henoux & Vogt 1998).

For coronal sources, under the assumption of a constant density coronal loop, temporal characteristics of the acceleration process can be deduced using the results of Sect. 4.4. The interesting aspect of this result is that the (square of the) width of the time profile of the HXRs is composed of two terms: the (square of the) width of the time profile of the injection plus a term proportional to $\tau(\epsilon)$ (squared). $\tau(\epsilon)$ is the collisional stopping time for an electron of energy equal to the photon energy of interest, ϵ, and is proportional to $\epsilon^{3/2}$. The peak of the HXR burst is also delayed with respect to the peak of injection by a time proportional to $\tau(\epsilon)$. These results can either be applied to the whole observed time profile of a Hard X-ray burst, or to the individual "spikes" of which it is composed. They should be useful in the time of flight analyses performed by Aschwanden and co-authors (Aschwanden et al. 1997 and references therein).

Acknowledgements. I would like to thank Alec MacKinnon, for insightful comments regarding the physical interpretation of the results, and Nicole Vilmer for valuable comments on their relevance to observations. I also thank the referee, Don Melrose, for his comments on the manuscript.

References

Alexander D., Metcalf T.R., 1997, ApJ 489, 442
Aschwanden M.J., Schwartz R.A., Dennis B.R., 1997, ApJ 502, 1
Bai T., 1982, ApJ 259, 341
Brown J.C., 1971, Sol. Phys. 18, 489
Brown J.C., Smith D.F., 1980, Rep. Prog. Phys. 43, 125
Brown J.C., Karlicky M., Mandzhavidze N., Ramaty, R., 2000, ApJ, in press
Conway A.J., MacKinnon A.L., Brown J.C., MacArthur G.K., 1998, A&A 331, 1103
Conway A.J., MacKinnon A.L., 1998a, In: Priest E., Moreno-Insertis F., Harris R. (eds.) A Crossroads for European Solar and Heliospheric Physics. p. 235

Conway A.J., MacKinnon A.L., 1998b, A&A 339, 298
Conway A.J., 2000, In: Mandzhavidze N., Ramaty R. (eds.) High Energy Solar Physics - Anticipating HESSI. ASP 206, p. 276
Craig I.J., Brown J.C., 1976, Ap&SS 149, 239
Craig I.J., MacKinnon A.L., Vilmer N., 1985, A&A 116, 251
Emslie A.G., 1978, ApJ 224, 241
Hamilton R.J., Lu E.T., Petrosian V., 1990, ApJ 354, 726
Henoux J.-C., Vogt E., 1998, Physica Scripta T78, 60
Karlicky M., 1997, Space Sci. Rev. 81, 143
Karlicky M., Brown J.C., Conway A.J., Penny G., 2000, A&A 353, 729
Kovalev V.A., Korolev O.S.. 1981, ApJ; SvA 25, 215
Leach J., Petrosian V., 1981, ApJ 251, 781
MacKinnon A.L., Brown J.C., 1989, Solar Phys. 122, 303
MacKinnon A.L., Craig I.J., 1991, A&A 251, 693
Masuda S., 1994, Ph.D. Thesis, University of Tokyo
Masuda S., Kosugi T., Hara H., et al., 1995, PASJ 47, 677
Miller J., Cargill P., Emslie A.G., et al., 1997, JGR 102, 14631
Ramaty R., Mandzhavidze N., Koslovsky B., Murphy R.J., 1995, ApJ 455, L193
Spitzer L., 1962, Physics of Fully Ionized Gases. John Wiley & Sons, p. 131
Trottet G., Vilmer N., Barat C., et al., 1998, A&A 334, 1099
Vilmer N., Trottet G., MacKinnon A.L., 1986, A&A 156, 64
Wheatland M.S., Melrose D.B., 1995, Solar Phys. 158, 283